

Article

In Situ Fabrication and Static Contact Resistance of CdMoO₄ Reinforced Cu Matrix Composites

Wei-Jian Li ¹, Lu Zhang ², Zi-Yao Chen ², Wen-Zhu Shao ^{2,3,*} and Liang Zhen ²¹ College of Nuclear Equipment and Nuclear Engineering, Yantai University, Yantai 264005, China² School of Materials Science and Engineering, Harbin Institute of Technology, Harbin 150001, China³ National Key Laboratory of Precision Hot Processing of Metals, Harbin Institute of Technology, Harbin 150001, China

* Correspondence: wzshao@hit.edu.cn

Abstract: Particle-reinforced Cu-based electrical contact materials prepared by traditional powder metallurgical methods suffer the same critical problem, where the agglomeration of the addition phases in the Cu matrix significantly deteriorates the performance of the composites and restricts their application. In this work, CdMoO₄/Cu matrix composites were fabricated by an in situ method and followed by a powder metallurgical process. Firstly, CdMoO₄/particles formed a nucleus and grew up based on the surfaces of Cu particles, realizing the controllable in situ synthesis of mixed powders with homogeneously dispersed CdMoO₄ nanoparticles via a one-step reaction. Secondly, the bulk CdMoO₄/Cu composites were fabricated by pressing and sintering and then densified by hot-extrusion and cold rolling processes. The microstructures and properties of the extruded and rolled specimens were characterized, respectively. The results indicated that the rolled CdMoO₄/Cu composite exhibited excellent comprehensive properties of electrical conductivity and mechanical properties for electrical contact materials. Moreover, the effects of the contact force on the static contact resistance of the extruded and rolled composites were evaluated in the closed state of the contact materials. It was found that the rolled CdMoO₄/Cu contact materials possessed a stable electrical contact characteristic with low and steady contact resistance. This work designed ternary CdMoO₄ particles to reinforce Cu-based composites with well-balanced performances by an in situ synthesis method and this strategy can be extended to the design of ternary oxide/metal composites utilized as electrical contact materials.

Keywords: Cu matrix composite; CdMoO₄; in situ synthesis; static contact resistance

Citation: Li, W.-J.; Zhang, L.; Chen, Z.-Y.; Shao, W.-Z.; Zhen, L. In Situ Fabrication and Static Contact Resistance of CdMoO₄ Reinforced Cu Matrix Composites. *Materials* **2022**, *15*, 7206. <https://doi.org/10.3390/ma15207206>

Academic Editor: Jie Zhou

Received: 19 September 2022

Accepted: 13 October 2022

Published: 16 October 2022

Publisher's Note: MDPI stays neutral with regard to jurisdictional claims in published maps and institutional affiliations.



Copyright: © 2022 by the authors. Licensee MDPI, Basel, Switzerland. This article is an open access article distributed under the terms and conditions of the Creative Commons Attribution (CC BY) license (<https://creativecommons.org/licenses/by/4.0/>).

1. Introduction

Copper is an attractive candidate to supersede precious metals utilized as electrical contact materials due to low cost and known superior electrical and thermal properties [1–3]. To satisfy the design requirements of electrical contact materials, numerous ceramic particles, such as Al₂O₃ [4], TiO₂ [5], and ZrO₂ [6], are generally introduced in the copper matrix to improve mechanical strength, wear, and arc resistance. However, the issue of inhomogeneous distribution of ceramic particles in the Cu matrix inevitably occurs in traditional preparation technologies, which significantly deteriorates the mechanical properties of Cu-based composites and limits their applications. To address this issue, an in situ method has aroused enormous interest and emerged as an effective route to synthesize dispersion-strengthened Cu-based composites. So far, extensive efforts have been dedicated to prepare TiO₂/Cu [7], TiB₂/Cu [8,9], and Al₂O₃/Cu [10] composites by an in situ method. The results indicated that the structures of the ceramic particle-reinforced Cu-based composites obtained by an in situ method were significantly improved with homogeneously distributed ceramic particles, and especially, these composites were proved to exhibit well-balanced electrical conductivity and mechanical properties.

Although the microstructures and properties of these oxide-reinforced Cu composites have been improved, the strong interfacial bonding of phase interfaces was still a major challenge due to the completely different characteristics of the constituents. When subjected to the impacts from the frictional force, the cyclic loading, and the impact force, on one hand, the weak bonding between ceramic particles and the Cu matrix could easily induce crack initiation and propagation, resulting in serious failure of these traditional composites [11–13]. On the other hand, the weak interfacial adhesion provides a diffusion path for oxygen, leading to the internal oxidation of the Cu matrix at high temperatures. Additionally, under arc erosion, the reinforcement particles tend to agglomerate on the contact surface, which is ascribed to the weak adhesion between reinforcement and Cu [14–17]. The agglomeration phenomenon gives rise to the increasing of contact electrical resistivity and temperature, resulting in failure of contact material during long-time arc erosion. As a consequence, the design of durable Cu matrix electrical contact materials has aroused extreme interest.

In comparison to the binary ceramic phase, the ternary compound possesses potential application in electrical contact materials due to its strong adherence to the metal matrix. For example, a $M_{n+1}AX_n$ phase such as Ti_3AlC_2 and Ti_3SiC_2 has been added in Cu matrices, which exhibited excellent arc-resistance performance [18–21]. A Zn_2SnO_4/Cu composite has been proved to decrease the mass loss under arc discharges, which was contributed to the strong ionic bonds across the phase interfaces [22]. In addition, Guo et al. [23] prepared Cu-based electrical contact materials reinforced by La_2NiO_4 , which decreased the contact resistance to 21.6 m Ω from 29.5 m Ω for pure Cu, and simultaneously, the temperature rises of the designed La_2NiO_4/Cu degraded significantly due to the separation of oxides under arc erosion. However, so far, ternary compound-reinforced Cu-based composites applied in electrical contact material are quite limited. For example, the Ti_3SiC_2/Cu electrical contact materials were mainly utilized in the condition of vacuum [24]. For the La_2NiO_4/Cu composite, it claimed that the addition of La_2NiO_4 led to a serious mass loss in contrast to the pure Cu due to the self-cleaning functions [23]. As a result, the Ag/CdO and Cu/CdO contact materials remain used in aerospace industries, and even in domestic applications [25]. Thus, achieving highly reliable non-previous metal composites subjected to arc erosion in air is always full of challenge and significance.

Combining the composition design and structure regulation, we describe an in situ approach to directly produce the $CdMoO_4/Cu$ composite. Here, $CdMoO_4$, exhibiting a combination characteristic of CdO as an arc-extinguishing agent and MoO_3 as flame retardant, is proposed and expected to tailor the properties of Cu-based composite. Importantly, the introduction of MoO_3 , as the constituent of ternary oxides, can remarkably decrease the content of CdO in the composite. Simultaneously, $CdMoO_4/Cu$ mixed powders were synthesized with a one-step process by an co-precipitation method, expecting to improve the dispersion degree of reinforcement phases and enhance their adherence to the metal matrix. Unlike a previous in situ method, in which the metal is easily to be oxidized in acid solution and need to be reduced by hydrogen, the neutral conditions for $CdMoO_4$ could protect Cu powders from oxidizing in solution.

In this work, to solve the problems of agglomeration and poor dispersion of the addition particles in the composites, we designed an in situ method with a one-step reaction to synthesize $CdMoO_4/Cu$ mixed powders, by which the $CdMoO_4$ could homogeneously nucleate and grow on the surface of Cu particle to enhance the adhesion of phase interface. After pressing and sintering, hot-extrusion and cold rolling processes were employed to improve the properties, including density, electrical conductivity, and mechanical properties of 2 wt.% $CdMoO_4/Cu$ composites, and especially, realize the industrial production for the Cu-based electrical contact materials. To estimate the electric contact characteristic of the designed electrical contact materials, the static contact resistances were measured and the effects of the mechanism of the contact force on the static contact resistance of $CdMoO_4/Cu$ were investigated. The purpose of this work is providing a simple and effective strategy for Cu-based composites with homogeneously distributed $CdMoO_4$ nanoparticles, and the

strategy can be extended to other ternary oxide reinforced Cu-based composites to enlarge their applications.

2. Experimental

2.1. Fabrication of CdMoO_4/Cu Mixed Powders and Composites

CdMoO_4/Cu mixed powders were fabricated as follows (Figure 1a): 0.03 mol of $\text{Na}_2\text{MoO}_4 \cdot 2\text{H}_2\text{O}$ and 0.06 mol of NaCl were added in 150 mL deionized water, and followed by adding 200 g electrolytic Cu powders (20~40 μm). The mixture was stirred continuously to form a suspension. Then, 0.03 mol $\text{CdCl}_2 \cdot 2.5\text{H}_2\text{O}$ were dissolved into 150 mL deionized water to get a clear solution. After that, the CdCl_2 solution were mixed with the above suspension under continually stirring for 10 min. Finally, the powder particles in solution were filtrated and repeatedly washed. Subsequently, the 2 wt.% CdMoO_4/Cu composites were prepared by powder metallurgy (Figure 1b–d), where 200 g electrolytic Cu powders were added in the dried CdMoO_4/Cu powders. Here, such a content of CdMoO_4 was promised to ensure a connected backbone structure of the Cu matrix, which, in view of the percolation theory [26,27], could provide transport paths for electric current. Excess CdMoO_4 would completely encase the Cu particles and deduce the electrical and thermal conductivity by decreasing the percolation backbone density of Cu. After mixing (see reference [2]), the mixed powders were compacted under 250 MPa, and then green compact with a diameter of 80 mm was sintered at 910 $^\circ\text{C}$ in Argon atmosphere for 45 min. Then, the columnar specimen was processed into plate (6 \times 50 mm^2) by hot extruding at 800 $^\circ\text{C}$. Afterwards, the rod material was cold rolled to a belt shape CdMoO_4/Cu composite with a thickness of 2 mm, and then annealed at 500 $^\circ\text{C}$ for 30 min.

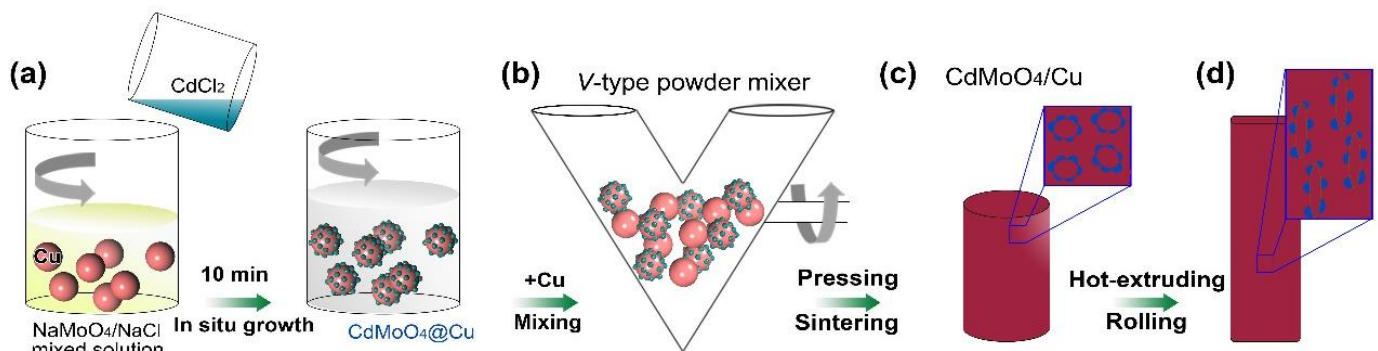


Figure 1. Schematic diagram of the fabrication of (a) CdMoO_4/Cu mixed powders by an in situ method and (b–d) CdMoO_4/Cu composites by powder metallurgy.

2.2. Characterizations

Five specimens with sizes of $2 \times 10 \times 10 \text{ mm}^3$ were cut from the composites and used for the measurement of the real density and hardness. The relative density of the composites calculated by dividing the theoretical density into the real density, and the real density was measured based on Archimedes principle. The hardness measurement was carried on a Vickers hardness tester (HV-1000A, Hua Yin Test Instrument Co., Ltd., Yantai, China), and ten positions were chosen for each sample and the hardness was achieved by averaging the testing values. Five specimens in the sizes of $2 \times 2 \times 60 \text{ mm}^3$ were cut from the plates along the extrusion and rolling directions, respectively and were used to measure the electrical conductivity by the four-probe method (Keithley 2420, Tektronix Inc., Beaverton, OR, USA) which was expressed in %IACS (International Annealed Copper Standard). Three samples for tensile testing with a gauge length of 18 mm and a cross-section of $1.5 \times 6 \text{ mm}^2$ were cut from the plates along the extrusion and rolling directions, respectively. Tensile tests were conducted at a strain rate of $5.6 \times 10^{-4} \text{ s}^{-1}$ using a universal testing machine (Instron-5569R, Boston, MA, USA) at room temperature, and the tensile test results were achieved by averaging the testing values. The static contact resistance was measured by mean of low-voltage alternating current contactor [2] installed with

four CdMoO_4/Cu specimens as movable and stationary contact materials, respectively. The adjustment of the gap distance between the contacts can realize the change of the contact force. Under a certain contact force, the static contact resistance can be achieved by the device of the simulation system with a four-probe method.

X-ray diffraction (D/Max 2500 system, Rigaku, Japan) was used to analyze the phases and structure of CdMoO_4/Cu powders. The scanning electron microscope (SEM) observation of the morphologies of the mixed powders and the fracture of the CdMoO_4/Cu composites was implemented on FEI Quanta 200F microscope (Waltham, MA, USA). Here, the sizes of CdMoO_4 particles and the grain were measured in Photoshop according to the ruler. The structure of the composites was characterized with metallographic microscope (Axiovert 40 MAT, Zeiss, Oberkochen, Germany).

3. Results and Discussion

3.1. Characterization of the CdMoO_4/Cu Mixed Powders and Composites

The morphologies of the raw Cu powders and as-prepared CdMoO_4/Cu powders, together with the XRD pattern of the obtained product, are shown in Figure 2. The dendritic morphology of the raw Cu in Figure 2a can provide large surface area for the growth of CdMoO_4 . After the in situ reaction, CdMoO_4 particles with the sizes of 550–650 nm distributed uniformly on the surface of Cu powders (Figure 2b), especially between the branches of the Cu powders, as shown in the regions of red circles. The result shows that the in situ method can effectively solve the agglomeration of the CdMoO_4 particles to ensure a uniform structure of the composite. High-magnification SEM image in Figure 2b shows that the CdMoO_4 particles synthesized by an in situ method were hemispherical morphology, indicating strong adhesion to the Cu powder. Simultaneously, it can be observed that there exist gaps among the CdMoO_4 particles without completely encasing the Cu powder as expected, which is beneficial to guarantee the electrical conductivity of the designed composites by forming continuous metallic passage. Additionally, Figure 2c shows that all diffraction peaks of the as-synthesized powders correspond to these of CdMoO_4 (JCPDS no. 07-0209) and Cu (JCPDS no. 04-0836) without any impurities.

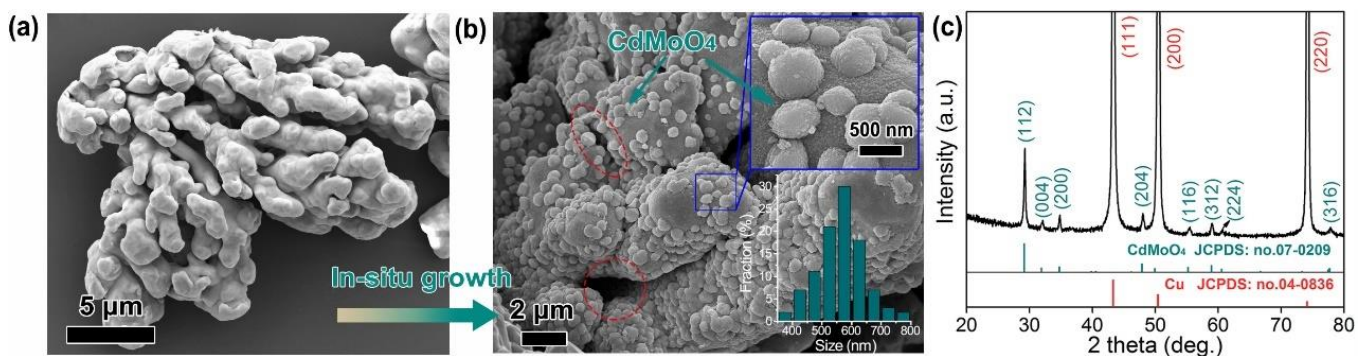


Figure 2. SEM images of (a) raw Cu powders and (b) as-synthesized CdMoO_4/Cu mixed powders. (c) XRD pattern of the CdMoO_4/Cu mixed powders. The inset in (b) is the high-magnification SEM image of CdMoO_4/Cu mixed powders and corresponding size distribution diagrams for CdMoO_4 particles.

Figure 3 shows the optical microstructures of CdMoO_4/Cu composites, which were etched by FeCl_3 solution. In Figure 3a, the grain size of extruded composite is approximately 10 μm. It can be detected that the CdMoO_4 particles were distributed at the grain boundaries, while some of them are embedded in the grain interior, as shown in the reign of red dashed circles. It needs to point that the black region in Figure 3 indicates the peeling of the CdMoO_4 particles from the composite surface after polishing. After rolled (Figure 3b), CdMoO_4 were distributed homogeneously, including the grain interior and grain boundary. The CdMoO_4 particles embedded in the grain interior are expected to improve the strength

of the composite by hindering the movement of dislocations. Notably, the grain of the CdMoO_4/Cu composites was obviously refined to approximately $5\ \mu\text{m}$ by a rolling process, and the grain refinement can also contribute to the improvement of the strength of the CdMoO_4/Cu composite. Moreover, the porosity, as a defect in the composites prepared via a powder metallurgical method, is one of the most important physical performance indexes, and excessive porosities could degrade the mechanical property and arc-resistance properties for the composites acting as electrical contact material. The relative densities (see Table 1) of the prepared composites were measured to be $99.0 \pm 0.4\%$ and $98.7 \pm 0.6\%$ for extruded and rolled specimens, respectively, which were significantly higher than those of reported ceramic/Cu [28,29] and [30,31] composites with the relative densities listed in Table 1. It reveals that the preparation technology involved in this work can effectively improve the density and decrease the porosity of the composites, which is the fundamental assurance of high reliability for electrical contact materials in practical applications.

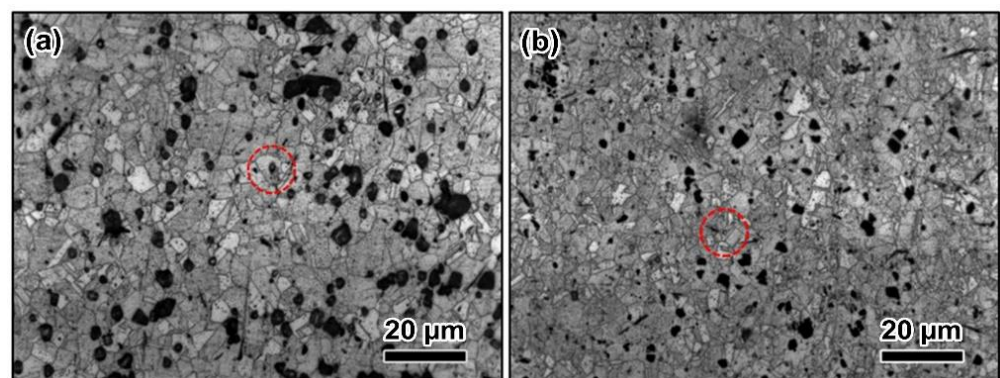


Figure 3. Optical images of the CdMoO_4/Cu composites by powder metallurgy: (a) the hot-extrusion state and (b) the rolling state. CdMoO_4 particles are indicated by red dashed circles.

Table 1. Relative density and electrical conductivity of CdMoO_4 -reinforced Cu-based composites.

	Relative Density (%)	Electrical Conductivity (%IACS)	Reference
Extruded specimen	99.0 ± 0.4	93.2 ± 1.1	This work
Rolled specimen	98.7 ± 0.6	89.1 ± 1.5	This work
3~9 wt.% ZrO_2/Cu	90.2~94.5	—	[28]
$\text{Ti}_3\text{SiC}_2/\text{Cu}$	92.52~95	—	[29]
10~12 wt.% $\text{Ti}_3\text{AlC}_2/\text{Ag}$	92.4~92.6	—	[30]
$\text{Ag}/\text{Ni}10$	91.8~98.6	—	[31]
2.5 wt.% TiO_2/Cu	—	78	[32]
2.75 wt.% $\text{Al}_2\text{O}_3/\text{Cu}$	—	85	[33]
2.5 wt.% $\text{Y}_2\text{O}_3/\text{Cu}$	—	37.8	[34]
5 wt.% $\text{La}_2\text{NiO}_4/\text{Cu}$	—	85	[23]

3.2. Electrical Properties

The electrical conductivity of the extruded CdMoO_4/Cu composite was measured to be $93.2 \pm 1.1\%$ IACS; however, the rolling technique cause a slight decrease on the electrical conductivity to a value of $89.1 \pm 1.5\%$ IACS. This highly relies on the changes of grain sizes discussed above, where electron scattering is slightly enhanced by the increasing grain boundary [35,36]. Nevertheless, the measured electrical conductivity is still higher than that of TiO_2/Cu [32], $\text{Al}_2\text{O}_3/\text{Cu}$ [33], $\text{Y}_2\text{O}_3/\text{Cu}$ [34], and $\text{La}_2\text{NiO}_4/\text{Cu}$ [23] electrical contact materials with values in the range of 34.7~85%IACS. The results reveal that the continuous metallic matrix in CdMoO_4/Cu composites provides a pathway for electrical conduction, which fulfills the performance demands of contact materials.

3.3. Mechanical Properties

The hardness of the extruded and rolled specimens was tested and is listed in Table 1. In comparison of the rolled specimen, the extruded CdMoO_4/Cu composite presents a relative lower hardness of $83.6 \pm 3.4 \text{ HV0.1}$, from which it can be speculated that welding could easily occur between movable and stationary contact materials and thus, two contacts fail to disconnect under arc erosion. However, when the composite was further processed with cold rolling, the hardness of the composite was obviously increased $103.5 \pm 1.8 \text{ HV0.1}$, which is ascribed to the CdMoO_4 embedded in the grain interior and the grain refinement caused by cold rolling. Additionally, the measured results with small error bar can reflect a uniform structure of the rolled CdMoO_4/Cu composite.

Figure 4 depicts the strain-stress curves of the extruded and rolled CdMoO_4/Cu composites and the performance metrics are listed in Table 2. It reveals that the yield strength ($245.9 \pm 6.2 \text{ MPa}$) of the rolled composite is 145% higher than that of extruded composite ($100 \pm 3.7 \text{ MPa}$). Compared with the tensile strength of extruded composite ($232.7 \pm 5.7 \text{ MPa}$), the tensile strength of the rolled composite increases slightly to $261.8 \pm 9.8 \text{ MPa}$. Except for the strength that decides the wear resistance and impact resistance during arc erosion, suitable ductility can ensure the factual contact area between the movable and stationary contact materials. The elongation of the extruded specimen is found to be $29.5 \pm 0.9\%$, close to the values from previous studies (32–35.7%) [2,7,37]. It can be deduced that the in situ synthesized CdMoO_4/Cu composites possess the ability of coordinate deformation, which is ascribed to the good interfacial coherent between CdMoO_4 and the Cu matrix. Note that, unlike the previous studies where the mechanical properties were improved except for the ductility, the elongation of the CdMoO_4/Cu composite increases from 29.5 ± 0.9 to $33.9 \pm 0.8\%$ after a rolling process, accompanying with the increasing of yield strength and tensile strength. This highly depends on the refined grains by a rolling process, which is consistent with the observation of the microstructure of the rolled composite. This testing was repeated at least three times, and same phenomena were achieved for the extruded and rolled CdMoO_4/Cu specimens. The results indicate that the mechanical performance, especially for the ductility, of the composites was remarkably improved by the CdMoO_4 particles by in situ fabrication.

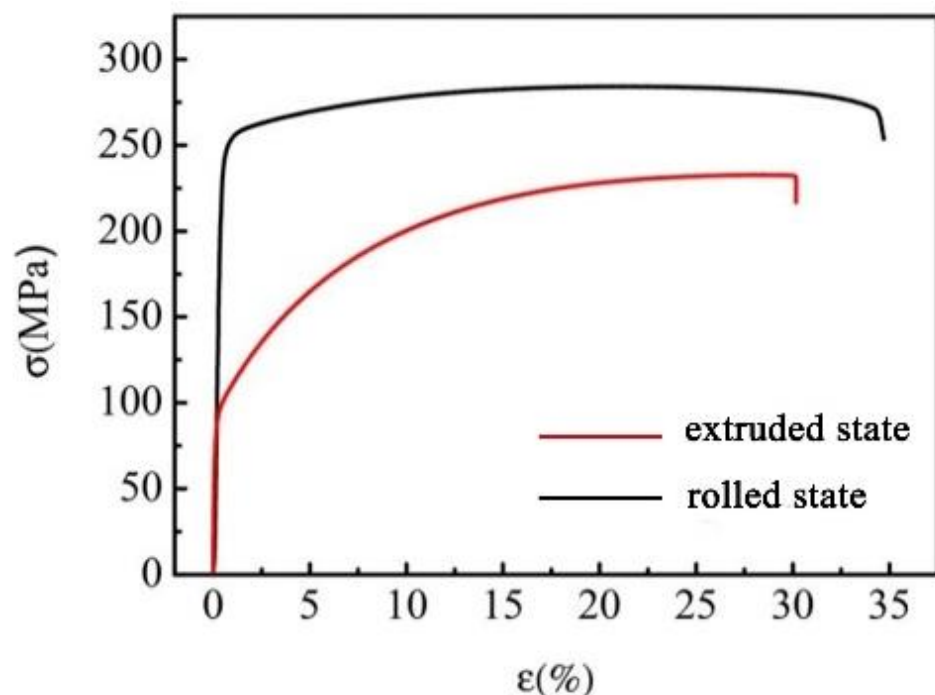
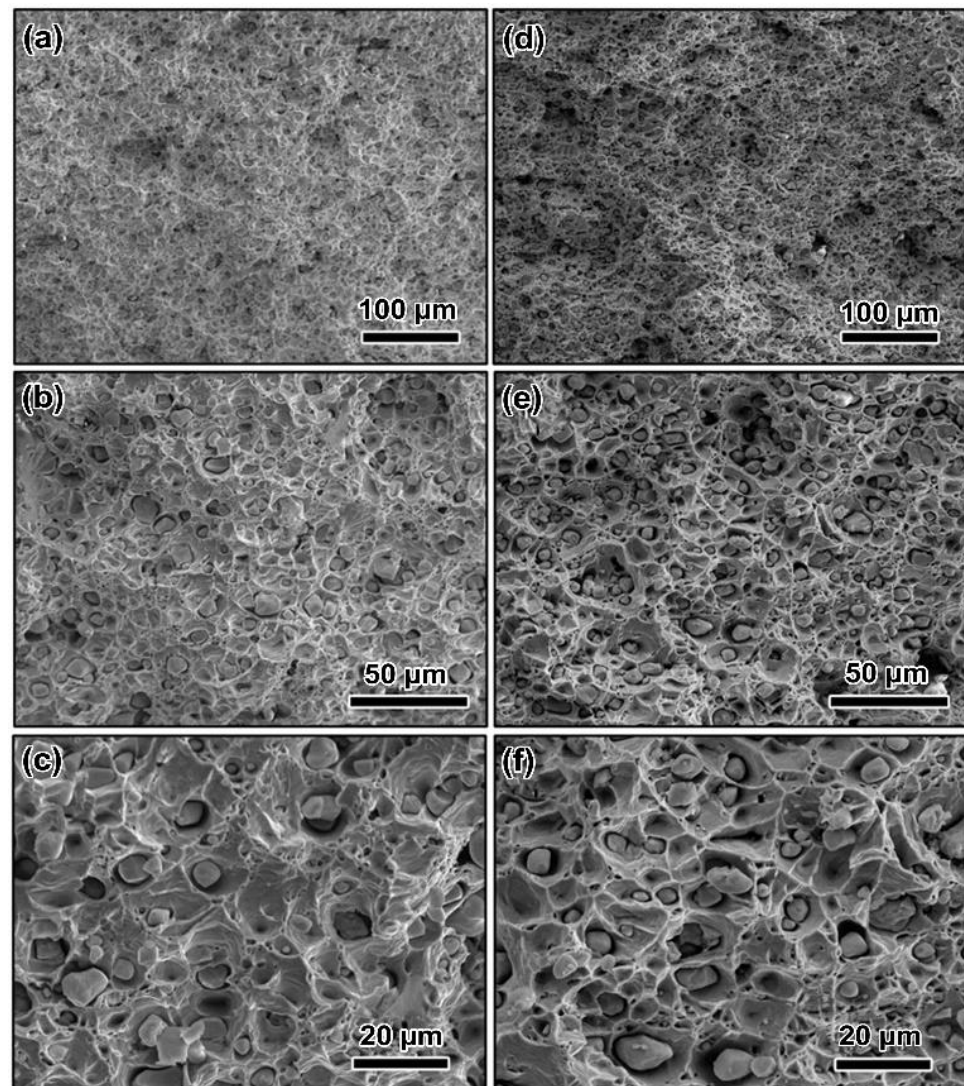


Figure 4. Strain-stress curves of extruded and rolled CdMoO_4/Cu composites.

Table 2. Mechanical properties of CdMoO₄-reinforced Cu-based composites.

	Hardness (HV0.1)	Yield Strength (MPa)	Tensile Strength (MPa)	Elongation (%)	Reference
Extruded specimen	83.6 ± 3.4	100.0 ± 3.7	232.7 ± 5.7	29.5 ± 0.9	This work
Rolled specimen	103.5 ± 1.8	245.9 ± 6.2	261.8 ± 9.8	33.9 ± 0.8	This work
2 wt.% SnO ₂ /Cu	92.1	279.8	363.5	28.4	[2]
2 wt.% Zn ₂ SnO ₄ /Cu	103.8	289.4	369.2	35.7	[2]
0.82 wt.% TiO ₂ /Cu	117.8 ± 6	290	—	32	[7]
0.2~0.8 wt.% CNTs/CuTi	88.22~100.86	152~192	266~352	15.1~28.2	[37]

The fracture morphologies of the CdMoO₄/Cu composites are shown in Figure 5. The fracture behavior of the extruded composite reveals ductile properties with the evidence of large dimple-like fracture structure (Figure 5a,c,e). With regard to the rolled composite, smaller and deeper fracture dimples were generated, signifying that the rolling process increases the ductility of CdMoO₄/Cu composites. These results are well consistent with those of the testing resulting of the mechanical performances of the CdMoO₄/Cu composites.

**Figure 5.** SEM images of the fracture of the (a,c,e) extruded CdMoO₄/Cu composite and (b,d,f) the rolled CdMoO₄/Cu composite.

3.4. Static Contact Resistance

Static contact resistance is an important evaluation index that significantly impacts on the performance stability of contact materials under the connection state, and Figure 6 gives the static contact resistance of CdMoO₄/Cu composites as a function of the contact force. As demonstrated in this figure, similar features can be observed for the extruded and rolled CdMoO₄/Cu composites. Under the condition of the lower contact force (80 g), the two CdMoO₄/Cu composites exhibited high contact resistance (6.5 mΩ). With increasing of the contact force, the static contact resistance of the composites decreased sharply until the contact force reached to 90 g, and then, the contact resistance decreased slowly. Finally, the contact resistances maintained stability in spite of the increasing of the contact force between the two contact materials. Note that, the electrical contact characteristic of rolled CdMoO₄/Cu specimen enter the steady state rapidly under the contact force of 95 g, resulting in a lower contact resistance of 1.6 mΩ, in comparison with that (2.5 mΩ) of the extruded specimen (100 g). It indicated that the CdMoO₄/Cu composite after rolling exhibited a more stable electrical contact characteristic, which is ascribed to excellent deformability for enlargement of the contact area. Additionally, the static contact resistance (1.6 mΩ) of the rolled CdMoO₄/Cu composites is close to the contact resistance (1.55 mΩ) Cu contact materials as reported [38], and especially, the contact resistance of the prepared CdMoO₄/Cu composites is lower than that of commercial Ag/CdO₁₂ (approximately 5 mΩ) [39] and Ag/12SnO₂ (approximately 1.6 mΩ) [40] electrical contact materials.

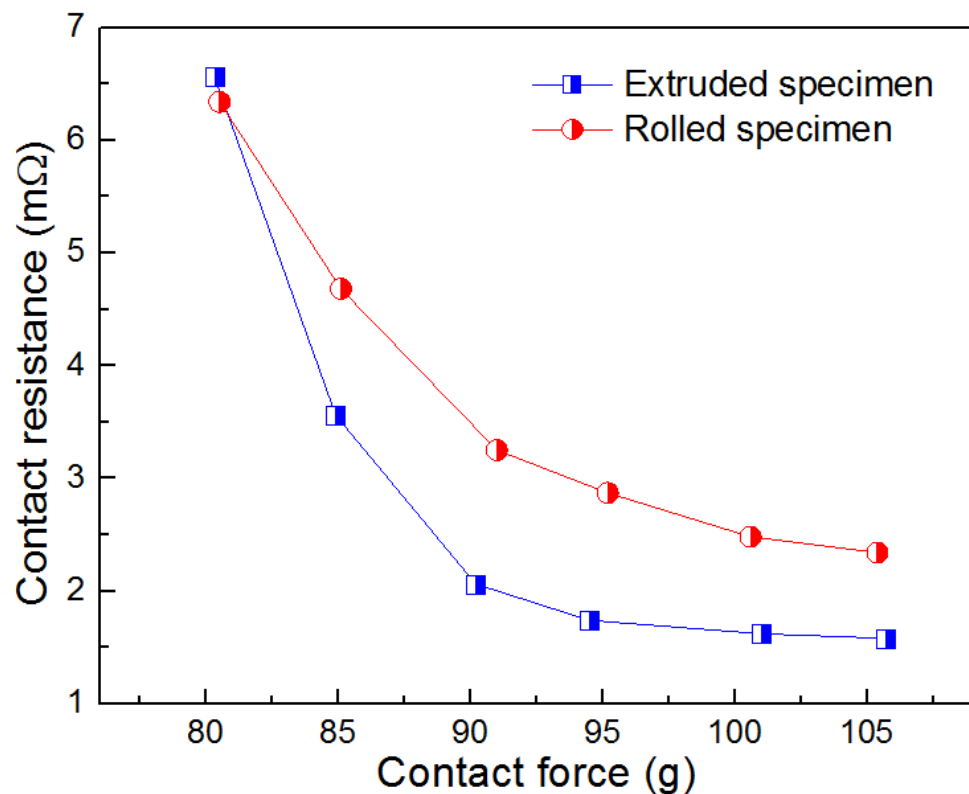


Figure 6. Changes of static contact resistance of CdMoO₄/Cu composites with the contact force.

Figure 7 illustrate the schematic demonstration of the variation of the contact resistance with the contact force, which can be generally divided into three stages according to the dominant factors. First, under a low contact force (Figure 7a), the movable and stationary contact materials contact with their sharp protuberances due to the surface roughness. In this case, the current contract, resulting in an increasing of the flow path of the current, and thus, additional resistance, namely shrinkage resistance, is generated at the contact sites. Simultaneously, the surface films containing oxidation film, impurity, and chemical

pollutants increase the contact resistance in the form of membrane resistance. At the second stage with an increased contact force (Figure 7b), these surface films were crushed by the contact force, decreasing the membrane resistance. Additionally, the contact area between the movable and stationary contact materials is enlarged and the shrinkage resistance is reduced. When further increasing the contact force (Figure 7c), sharp protuberances become flat, and the occurrence of work hardening leads to saturation point of the contact area [38], resulting in a stably contact resistance.

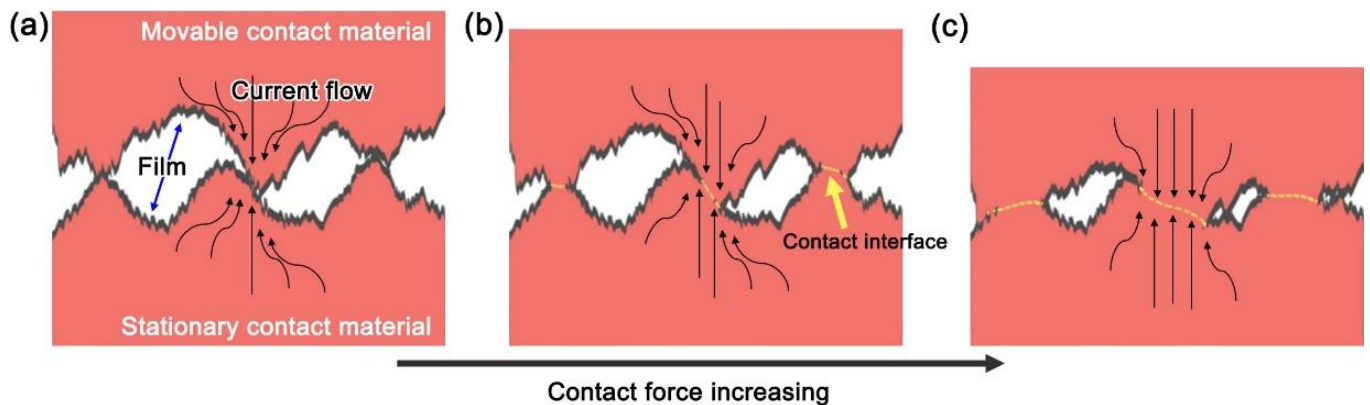


Figure 7. Schematic diagram of formation of contact resistance with increasing of the contact force. (a) Initial contact between the two contact materials, (b) Breakage of the film caused by increasing contact force, (c) Plastic deformation of the contact zone.

4. Conclusions

CdMoO₄/Cu composites were prepared by an in situ method and followed by a powder metallurgical method. The effects of processing technologies on the structures and properties of the CdMoO₄/Cu composites were investigated. The conclusions are as follows.

- (1) CdMoO₄/Cu mixed powders were successfully synthesized in a one-step reaction by an in situ method. The hemispherical CdMoO₄ particles with the sizes of 500 nm grew uniformly on the Cu powders, realizing the controllable synthesis for ternary CdMoO₄/Cu mixed powders with homogeneously dispersed reinforced phases. The proposed preparation method was determined to be a suitable technology for the particle-reinforced Cu-based composites.
- (2) The CdMoO₄/Cu composites were fabricated by a powder metallurgy method. In comparison with the extruded state of composite, the rolling process refined the grain from 10 to 5 μm and the CdMoO₄ particles embedded in the grain interior.
- (3) The rolled CdMoO₄/Cu composite was verified to possess excellent comprehensive performances of relative density (98.7 ± 0.6%), electrical conductivity (89.1 ± 1.5%), hardness (103.5 ± 1.8 HV0.1), yield strength (245.9 ± 6.2 MPa), tensile strength (261.8 ± 9.8 MPa), and elongation (33.9 ± 0.9%).
- (4) The variation tendencies of contact resistance of extruded and rolled CdMoO₄/Cu composites with the contact force were evaluated. Small contact area and surface film caused a large contact resistance (approximately 6.5 mΩ) under a low contact force. A large contact force was applied to break the film of the contact surface, sharply decreasing the contact resistances. When hardening occurred and the contact area reached a saturation state, the contact resistances maintained stability.
- (5) In comparison with the extruded specimen, the rolled CdMoO₄/Cu composite with lower contact resistance (1.6 mΩ) exhibited a more stable electrical contact characteristic, which is ascribed to excellent deformability for enlargement of the contact area. The designed CdMoO₄/Cu composite can be expected to use as electrical contact materials with a low and stable contact characteristic.

Author Contributions: Conceptualization, W.-Z.S.; Data curation, W.-J.L.; Formal analysis, L.Z. (Lu Zhang) and Z.-Y.C.; Funding acquisition, W.-J.L. and W.-Z.S.; Investigation, L.Z. (Lu Zhang); Project administration, L.Z. (Liang Zhen); Supervision, L.Z. (Liang Zhen); Visualization, Z.-Y.C.; Writing—original draft, W.-J.L.; Writing—review & editing, W.-Z.S. All authors have read and agreed to the published version of the manuscript.

Funding: This work was financially supported by National Natural Science Foundation of China, under grant Nos. 51371072 and 52201229.

Institutional Review Board Statement: Not applicable.

Informed Consent Statement: Not applicable.

Data Availability Statement: The data presented in this study are available on request from the corresponding author.

Conflicts of Interest: The authors declare no conflict of interest.

References

1. Zuo, H.; Wei, W.; Yang, Z.; Li, X.; Ren, J.; Xiao, Y.; Liao, Q.; Yin, G.; Gao, G.; Wu, G. Performance Enhancement of Carbon/Copper Composites based on Boron Doping. *J. Alloys Compd.* **2021**, *876*, 160213. [[CrossRef](#)]
2. Li, W.-J.; Chen, Z.-Y.; Jiang, H.; Sui, X.-H.; Zhao, C.-F.; Zhen, L.; Shao, W.-Z. Effects of Interfacial Wettability on Arc Erosion Behavior of Zn₂SnO₄/Cu Electrical Contacts. *J. Mater. Sci. Technol.* **2022**, *109*, 64–75. [[CrossRef](#)]
3. Zhang, X.; Zhang, Y.; Tian, B.; An, J.; Zhao, Z.; Volinsky, A.-A.; Liu, Y.; Song, K. Arc Erosion Behavior of the Al₂O₃-Cu/(W, Cr) Electrical Contacts. *Compos. Part B* **2019**, *160*, 110–118. [[CrossRef](#)]
4. Rajesh, K.-L.; Amirthagadeswaran, K.-S. Corrosion and Wear Behaviour of Nano Al₂O₃ Reinforced Copper Metal Matrix Composites Synthesized by High Energy Ball Milling. *Part. Sci. Technol.* **2020**, *38*, 228–235.
5. Moghanian, A.; Sharifianjazi, F.; Abachi, P.; Sadeghi, E.; Jafarikhorami, H.; Sedghi, A. Production and Properties of Cu/TiO₂ Nano-Composites. *J. Alloy. Compd.* **2017**, *698*, 518–524. [[CrossRef](#)]
6. Ding, J.; Zhao, N.; Shi, C.; Du, X.; Li, J. In Situ Formation of Cu-ZrO₂ Composites by Chemical Routes. *J. Alloy. Compd.* **2006**, *425*, 390–394. [[CrossRef](#)]
7. Han, T.; Li, J.; Zhao, N.; Shi, C.; Liu, E.; He, F.; Ma, L.; Li, Q.; He, C. In-Situ Fabrication of Nano-Sized TiO₂ Reinforced Cu Matrix Composites with Well-Balanced Mechanical Properties and Electrical Conductivity. *Powder Technol.* **2017**, *321*, 66–73. [[CrossRef](#)]
8. Jiang, Y.; Han, L.; Xu, Y.; Cao, F.; Du, X.; Han, F.; Cai, L.; Zhu, J. Arc Erosion Behaviour of In-Situ TiB₂/Cu Composites with a Three-Dimensional Network Structure. *Mater. Res. Express* **2022**, *9*, 046503. [[CrossRef](#)]
9. Qiu, F.; Duan, X.; Dong, B.; Yang, H.; Lu, J.; Li, X. Effects of Cr and Zr Addition on Microstructures Compressive Properties and Abrasive Wear Behaviors of In Situ TiB₂/Cu Cermets. *Materials* **2018**, *8*, 1464. [[CrossRef](#)]
10. Shen, Y.; Zhu, J.; Xu, Y.; Wang, B.; Li, T. Fabrication of an In-Situ Nano-Al₂O₃/Cu Composite with High Strength and High Electric Conductivity. *Rare Met.* **2005**, *24*, 46–54.
11. Zhang, X.; Hong, C.; Han, J.; Zhang, H. Microstructure and Mechanical Properties of TiB₂/(Cu, Ni) Interpenetrating Phase Composites. *Scr. Mater.* **2006**, *55*, 565–568. [[CrossRef](#)]
12. Yang, Z.; Zhou, Y.; Wang, T.; Liu, Q.; Lu, Z. Crack Propagation Behaviors at Cu/SiC Interface by Molecular Dynamics Simulation. *Comput. Mater. Sci.* **2014**, *82*, 17–25. [[CrossRef](#)]
13. Han, J.; Hong, C.; Zhang, X.; Wang, B. Thermal Shock Resistance of TiB₂-Cu Interpenetrating Phase Composites. *Compos. Sci. Technol.* **2005**, *65*, 1711–1718. [[CrossRef](#)]
14. Zhao, W.-J.; Wang, J.-B.; Wang, R.-J.; Wang, Y.-L.; Liu, S.-T.; Hu, Z.-T. Influence of Doping on Properties of Cu/SnO₂ Contact Materials. *J. Aeronaut. Mater.* **2015**, *35*, 60–64.
15. Chen, P.; Wang, Y. Improved Arc Erosion Resistance of Ag/SnO₂ Composites Fabricated by Ag Melt-Infiltration in the SnO₂ Skeleton. *Mater. Lett.* **2022**, *310*, 131520. [[CrossRef](#)]
16. Chen, Z.-Y.; Shao, W.-Z.; Li, W.-J.; Sun, X.-Y.; Zhen, L.; Li, Y. Suppressing the Agglomeration of ZnO Nanoparticles in Air by Doping with Lower Electronegativity Metallic Ions: Implications for Ag/ZnO Electrical Contact Composites. *ACS Appl. Nano Mater.* **2022**, *5*, 10809–10817. [[CrossRef](#)]
17. Güler, Ö.; Evin, E. The Investigation of Contact Performance of Oxide Reinforced Copper Composite via Mechanical Alloying. *J. Mater. Process. Technol.* **2009**, *209*, 1286–1290. [[CrossRef](#)]
18. Huang, X.; Feng, Y.; Li, L. Erosion Behavior of a Cu-Ti₃AlC₂ Cathode by Multi-Electric Arc. *Materials* **2019**, *12*, 2947. [[CrossRef](#)]
19. Wang, W.; Zhai, H.; Chen, L.; Zhou, Y. Sintering and Properties of Mechanical Alloyed Ti₃AlC₂-Cu Composites. *Mater. Sci. Eng. A* **2017**, *685*, 154–158. [[CrossRef](#)]
20. Zhang, R.; Liu, F.; Tulugan, K. Self-Lubricating Behavior Caused by Tribo-oxidation of Ti₃SiC₂/Cu Composites in a Wide Temperature Range. *Ceram. Int.* **2022**, *48*, 15504–15515. [[CrossRef](#)]

21. Jiang, X.; Liu, W.; Li, Y.; Shao, Z.; Luo, Z.; Zhu, D.; Zhu, M. Microstructures and Mechanical Properties of Cu/Ti₃SiC₂/C/Graphene Nanocomposites Prepared by Vacuum Hot-Pressing Sintering and Hot Isostatic Pressing. *Compos. Part B Eng.* **2018**, *141*, 203–213. [[CrossRef](#)]
22. Li, W.-J.; Shao, W.-Z.; Xie, N.; Zhang, L.; Li, Y.-R.; Yang, M.-S.; Chen, B.-A.; Zhang, Q.; Wang, Q.; Zhen, L. Air Arc Erosion Behavior of CuZr/Zn₂SnO₄ Electrical Contact Materials. *J. Alloy. Compd.* **2018**, *743*, 697–706. [[CrossRef](#)]
23. Guo, Y.-L.; Zhou, Z.-B.; Wang, Y.-P. Preparation, Electrical Contact Performance and Arc-Erosion Behavior of Cu/La₂NiO₄ Composites. In Proceedings of the 3rd International Conference on Material, Mechanical and Manufacturing Engineering (IC3ME 2015), Guangzhou, China, 27–28 June 2015; Atlantis Press: Paris, France, 2015; pp. 1532–1536.
24. Zhang, P.; Ngai, T.-L.; Wang, A.; Ye, Z.-Y. Arc Erosion Behavior of Cu-Ti₃SiC₂ Cathode and Anode. *Vacuum* **2017**, *141*, 235–242. [[CrossRef](#)]
25. Wu, Q.; Xu, G.; Yuan, M.; Wu, C. Influence of Operation Numbers on Arc Erosion of Ag/CdO Electrical Contact Materials. *IEEE Trans. Compon. Packag. Manuf. Technol.* **2020**, *10*, 845–857. [[CrossRef](#)]
26. Xie, N.; Shao, W.; Feng, L.; Lv, L.; Zhen, L. Fractal Analysis of Disordered Conductor–Insulator Composites with Different Conductor Backbone Structures near Percolation Threshold. *J. Phys. Chem. C* **2012**, *116*, 19517–19525. [[CrossRef](#)]
27. Feng, L.-C.; Xie, N.; Shao, W.-Z.; Lu, L.-X.; Zhen, L. Thermal Conductivity Determination of Conductor/Insulator Composites by Fractal: Geometrical Tortuosity and Percolation. *Compos. Part B.* **2016**, *92*, 377–383. [[CrossRef](#)]
28. Fathy, A.; Elkady, O.; Abu-Oqail, A. Synthesis and Characterization of Cu-ZrO₂ Nanocomposite Produced by Thermochemical Process. *J. Alloy. Compd.* **2017**, *719*, 411–419. [[CrossRef](#)]
29. Xie, H.; Ngai, T.-L.; Zhang, P.; Li, Y. Erosion of Cu-Ti₃SiC₂ Composite under Vacuum Arc. *Vacuum* **2015**, *114*, 26–32. [[CrossRef](#)]
30. Ding, J.; Tian, W.-B.; Zhang, P.; Zhang, M.; Zhang, Y.-M.; Sun, Z.-M. Arc Erosion Behavior of Ag/Ti₃AlC₂ Electrical Contact Materials. *J. Alloy. Compd.* **2018**, *740*, 669–676. [[CrossRef](#)]
31. Lin, Z.; Fan, S.; Liu, M.; Liu, S.; Li, J.-G.; Li, J.; Xie, M.; Chen, J.; Sun, X. Excellent Anti-Arc Erosion Performance and Corresponding Mechanisms of a Nickel-Belt-Reinforced Silver-based Electrical Contact Materials. *J. Alloy. Compd.* **2019**, *788*, 163–171. [[CrossRef](#)]
32. Sorkhe, Y.-A.; Aghajani, H.; Tabrizi, A.-T. Synthesis and Characterisation of Cu-TiO₂ Nanocomposite Produced by Thermochemical Process. *Powder Metall.* **2016**, *59*, 107–111. [[CrossRef](#)]
33. Zhang, X.-H.; Li, X.-X.; Chen, H.; Li, T.-B.; Su, W.; Guo, S.-D. Investigation on Microstructure and Properties of Cu-Al₂O₃ Composites Fabricated by a Novel In-Situ Reactive Synthesis. *Mater. Des.* **2016**, *92*, 58–63. [[CrossRef](#)]
34. Mu, Z.; Geng, H.-R.; Li, M.-M.; Nie, G.-L.; Leng, J.-F. Effects of Y₂O₃ on the Property of Copper based Contact Materials. *Compos. Part B* **2013**, *52*, 51–55. [[CrossRef](#)]
35. Sorkhe, Y.A.; Aghajani, H.; Tabrizi, A.-T. Mechanical Alloying and Sintering of Nanostructured TiO₂ Reinforced Copper Composite and Its Sharacterization. *Mater. Des.* **2014**, *58*, 168–174. [[CrossRef](#)]
36. Ding, C.; Xu, J.; Shan, D.; Guo, B.; Langdon, T.-G. Sustainable Fabrication of Cu/Nb Composites with Continuous Laminated Structure to Achieve Ultrahigh Strength and Excellent Electrical Conductivity. *Compos. Part B Eng.* **2021**, *211*, 108662. [[CrossRef](#)]
37. Xiong, N.; Bao, R.; Yi, J.; Fang, D.; Tao, J.; Liu, Y. CNTs/Cu-Ti Composites Fabrication through the Synergistic Reinforcement of CNTs and in situ Generated Nano-TiC Particles. *J. Alloy. Compd.* **2019**, *770*, 204–213. [[CrossRef](#)]
38. Timsit, R.-S. Electrical Contact Resistance: Properties of Stationary Interfaces. *IEEE Trans. Compon. Packag. Technol.* **1999**, *22*, 85–98. [[CrossRef](#)]
39. Ren, W.; Jian, W.; Yu, C.; Sheng, C.; Li, C.; Zhai, G. Precision Measuring Technique for Contact Resistance of Contact Materials. *Trans. China Electrotech. Soc.* **2014**, *29*, 31–35.
40. Leung, C.; Bourda, C. An Evaluation of Ag/W and Ag/Metal Oxide Arcing Contact Combinations for Circuit Breaker Applications. In Proceedings of the 27th International Conference on Electrical Contacts, Dresden, Germany, 22–26 June 2014; pp. 67–72.